EFFICIENT THREE-DIMENSIONAL BUILDING-SOIL MODEL FOR THE PREDICTION OF GROUND-BORNE VIBRATIONS IN BUILDINGS

Arnau Clot [1], Robert Arcos [2], Jordi Romeu [3]

ABSTRACT

This paper proposes a new efficient model for the prediction of low-amplitude ground-borne vibrations in buildings. The model takes into account the three-dimensional nature of the building structure by analytical and semi-analytical means, making it ideal for performing parametric studies or large-scale vibrations predictions. Its formulation assumes that the principal component in floor vibrations is the vertical one and assumes that the vibrations are transmitted to the various floors through the building columns. The correctness of the model is tested by comparing, in two three-story building examples, its results with those obtained using a numerical model. Results regarding the isolation efficiency of implementing a thicker lower floor or columns with a larger cross-section are also presented. The building-soil coupling is formulated considering piled foundations in a stratified soil. To ensure the computational efficiency of the calculations, the piles' response to an incident wavefield is modeled considering the Novak pile model for a layered half-space. Finally, a study of the importance of the soil mechanical parameters in the considered problem is conducted using the building-soil coupled model.

Keywords: Dynamic building model, Ground-borne vibrations, Layered half-space, Thin plate.

[1]Acoustical and Mechanical Engineering Laboratory (LEAM). Universitat Politècnica de Catalunya, Spain, E-mail:arnau.clot@upc.edu.

[2]Acoustical and Mechanical Engineering Laboratory (LEAM). Universitat Politècnica de Catalunya, Spain

[3]Acoustical and Mechanical Engineering Laboratory (LEAM). Universitat Politècnica de Catalunya, Spain

INTRODUCTION

Ground-borne vibrations, such as the ones induced by construction works or by the passing of trains and traffic, can cause annoyance to nearby building dwellers and, in the case of large strains, structural damage to building structures. A correct prediction of these vibrations allows deciding whether or not a particular vibration mitigation countermeasure should be applied either on the generation source, in the transmission path or on the receiver. These countermeasures have to take into account the frequency range of interest which ISO 2631-2 (2003) defines as 1-80 Hz, for the case of ground-borne vibrations in buildings, and 20-250 Hz, when information regarding the reradiated noise is also considered. The prediction of building vibrations has been attempted using different types of models, usually classified into three groups: empirical, numerical and (semi)analytical models.

Empirical models predict the ground-borne induced vibrations using simple decaying laws usually combined with experimental data from previous measurements. In the case of railway-induced vibrations, several empirical methods have been developed following the stage differentiation defined by ISO 14837-1 (2005). An example is the method presented by Kuppelwieser and Ziegler (1996), who developed a three-parts computer program with two prediction models - one rather simple and the other much more detailed - supplied by a database of vibration and noise measurements. A similar separation has been also proposed in the empirical models presented by Madshus et al. (1996) and by Hood et al. (1996), both also based on experimental measurements. A significant number of soil attenuation laws have been discussed in the works of Auersch (2010a, 2010b). An empirical model that also considers the building response was presented by Kurzweil (1979). A comprehensive review of prediction models for railway-induced vibrations, especially focused on empirical ones, has been recently presented by Lombaert et al. (2015). Empirical models, despite being computationally very efficient, exhibit limited accuracy.

Prediction models based on numerical methods are currently the only option for dealing in detail with the complex geometry of a building-soil system. Because the main disadvantage

of these models is their high computational cost, different types of approaches have been proposed in order to improve their efficiency. A two-dimensional (2D) Finite Element-Boundary Element (FE-BE) model for understanding the surface excitation of a building wall and foundation was proposed by Jean and Villot (2000). The model has been later extended to a two-and-a-half dimensional (2.5D) formulation and used to evaluate the influence of several building parameters (Villot et al. 2011). A three-dimensional (3D) FE-BE model was used by Fiala et al. (2007) to predict the ground-borne noise generated by surface rail traffic. The model, which solved the full problem as three weakly coupled subproblems, was later used to consider the noise generated by underground railways (Fiala et al. 2008). Lopes et al. (2014) have recently presented a complete building-soil model for the prediction of railway induced vibrations using submodeling techniques. However, despite the rapid increase of computers' computational power, numerical models are still not feasible for performing large-scale vibration predictions or certain parametric studies. In these cases, the use of a more efficient but still realistic type of prediction model is necessary.

A wide variety of analytical models (where the response is given by closed-form solutions) and semianalytical models (which require the numerical computation of complex analytical expressions) have been proposed to predict the building response to incident vibrations. Following the analytical approach proposed by Hudson (1956) in the field of seismology, Waller (1969) represented the building as a 1-degree of freedom (DOF) system. A similar type of building model has been more recently proposed by Auersch (2008), who studied the vertical building resonance adding the mass of the building to the dynamic stiffness of the ground. Newland and Hunt (1991) illustrated that this kind of approach was insufficient for accurately representing the complex response of a continuous structure and proposed the use of columns of infinite length for modeling the building. This type of approach has been recently used by Sanayei et al. (2012), who modeled the dynamic behavior of the building floors by adding the impedance of infinite thin plates to a finite column model. Cryer and Hunt (1994) considered the building as a 2D framed structure composed of horizontal and

vertical beams joined at their ends. The model was later used to perform predictions of the building response to railway induced vibrations (Hunt 1995). Talbot (2001) coupled the building model to a 3D BE model of the piled foundations for studying the dynamic response of base-isolated buildings. More recently, a prediction model that couples the previous frame structure to a layered soil and computes the response of this soil using the thin-layer method has been presented by Hussein et al. (2013). The authors are not aware of the existence of any 3D analytical model for the prediction of building vibrations.

The present work proposes a new efficient three-dimensional model for predicting low-amplitude ground-borne vibrations in buildings. The proposed model combines an acceptable accuracy of the predicted results with a small computational cost, making the model highly suitable for performing a wide variety of parametric studies and also large-scale vibration predictions. The model takes into account the 3D nature of a multi-story building and considers that the vibration is transmitted to the different floors through the building's columns. The model also considers that the building has piled foundations buried in a stratified soil.

The paper is structured as follows. First, the analytical formulation of the proposed model is described. Then, a numerical validation of the building model and the results obtained in the range of frequencies of interest in building vibrations are presented. Finally, the main conclusions of this work are highlighted.

BUILDING-SOIL MODEL FORMULATION

This section develops the formulation of the proposed building-soil model. A 3D diagram of the considered problem is presented in Fig. 1 (a), which represents a two-story building with six columns in each floor built on soil composed of two layers over a half-space. In general, the building-soil model considers a $(N_s + 1)$-story building (N_s stories over a ground level) with rectangular floors supported by a distribution of round columns. The building is constructed on stratified soil, which is assumed to be composed of N_L horizontal layers over a half-space. Piled foundations are considered for modeling the building-soil interaction.

The piles are buried in one or more of the soil layers and the whole system is excited by an external circular surface or buried vertical harmonic load $\mathbf{F}_{\text{out}}$. The soil layers and the building floors, columns and stories considered in this work are listed in Fig. 1 (b).

The dynamic response of the building floors is obtained once the coupling forces between the different parts of the complete system are determined. The coupling forces are considered to be vertical forces because it is assumed that the vertical component of the building vibrations is significantly more important than the horizontal ones. This assumption is in agreement with experimental measurements found in the literature (Sanayei et al. 2013; Athanasopoulos and Pelekis 2000; Crispino and D'Apuzzo 2001).

Floor and columns models

For the sake of simplicity it is considered that the columns are arranged in a $N_x \times N_y$ equispaced rectangular grid pattern. Therefore, a supporting column can be identified with a pair of indexes i and j, where $i = 1, \ldots, N_x$ and $j = 1, \ldots, N_y$, which indicate its position in the story, and an index k, where $k = 0, \ldots, N_s$, which indicates the considered story ($k = 0$ is the ground floor). Each of these columns is assumed to be an axial homogeneous and isotropic circular rod of constant cross-section A_c and height L_c (see Fig. 2 (a)). The external loads applied at the column edges are the coupling loads caused by the adjacent upper and lower floors. Following the story numbering scheme presented in Fig. 1 (b), the supporting column (i, j) of the k-story is excited by a force caused by its coupling with floor k and a force caused by its coupling with floor $k+1$. These two forces are labeled as $F_{i,j}^{2k}$ and $F_{i,j}^{2k+1}$, respectively. In the notation used in this work upper case letters are used to indicate that a variable is defined in the frequency domain.

The axial response of an elastic homogeneous rod of constant cross-section is described by

$$E_c \frac{\partial^2 u}{\partial z^2} = \rho_c \frac{\partial^2 u}{\partial t^2} \tag{1}$$

where E_c is the Young modulus of the column material and ρ_c is its density.

In the frequency domain, the vertical response of the column (i, j) in the story k to the coupling forces applied on its edges is given by

$$U_{i,j}^{k}(z) = C_0(z)F_{i,j}^{2k} + C_L(z)F_{i,j}^{2k+1}, \tag{2}$$

where z is the vertical position in the column local system of coordinates (see Fig. 2 (a)) and where C_0 and C_L are the column compliances to forces acting at the base and head of the column, respectively. These compliances can be expressed as

$$\begin{aligned} C_0(z) &= \frac{-1}{E_c A_c \beta}\left[\sin(\beta z) + \frac{\cos(\beta z)}{\tan(\beta L_c)}\right], \\ C_L(z) &= \frac{\cos(\beta z)}{E_c A_c \beta \sin(\beta L_c)}, \end{aligned} \tag{3}$$

where

$$\beta = \frac{\omega}{c_0}, \qquad c_0 = \sqrt{E_c/\rho_c}, \tag{4}$$

where ω is the angular frequency.

The floors are modeled as rectangular elastic homogeneous isotropic plates of constant width h_f and of lengths L_x and L_y (see Fig. 2 (b)). The ratio between the width and the other floor dimensions is assumed to be small, allowing the use of thin plate formulation. The deflection of the plate is given by

$$D_f \nabla^4 w + \rho_f \frac{\partial^2 w}{\partial t^2} = 0, \tag{5}$$

where ρ_f is the floor material density, ∇ is the nabla operator and where

$$D_f = \frac{E_f h_f^3}{12(1-\nu_f^2)}, \tag{6}$$

where E_f is the plate's Young modulus, h_f is its thickness and ν_f is its Poisson ratio.

The coupling forces between floor k and the adjacent lower and upper columns (columns $k-1$ and k, respectively) are assumed to be vertical point loads applied at the floor-column joint positions. In the frequency domain, the deflection W_k of floor k caused by its interaction with all the upper and lower columns is given by

$$W_k(x,y) = \sum_{i=1}^{N_x}\sum_{j=1}^{N_y}(F_{i,j}^{2k-1} - F_{i,j}^{2k})A(x,y;x_i,y_j), \tag{7}$$

where (x_i, y_j) is the position of the center of column (i,j) in the floor local system of coordinates and where $A(x,y;x_i,y_j)$ is the floor compliance at (x,y) to a force applied at (x_i,y_j), which can be expressed as

$$A(x,y;x_i,y_j) = \sum_{m=1}^{\infty}\sum_{n=1}^{\infty} W_{nm}(x,y)W_{nm}(x_i,y_j)B_{nm}, \tag{8}$$

where W_{nm} is the (n,m)-mode eigenfunction of the thin plate and where

$$\begin{aligned} B_{nm} &= \frac{\mathrm{e}^{\mathrm{i}\phi_{nm}}}{C_{nm}\rho_f h_f\sqrt{(\omega_{nm}^2-\omega^2)^2+\omega_{nm}^4\eta_f^2}}, \\ \phi_{nm} &= \arctan\left(\frac{\eta_f}{1-(\omega/\omega_{nm})^2}\right), \\ C_{nm} &= \int_0^{L_x}\int_0^{L_y}[W_{nm}(x,y)]^2\mathrm{d}y\mathrm{d}x, \end{aligned} \tag{9}$$

where η_f is the structural damping factor and ω_{nm} is the (n,m)-mode eigenfrequency. The lack of an exact expression for the free rectangular plate eigenmodes is overcome in this work by considering the results developed by Warburton (1954). Warburton used the Rayleigh-Ritz method to obtain approximate frequency formulas by assuming that the plate mode shapes are a product of two vibrating beam mode shapes. Because the free-edge conditions of a thin plate are not exactly satisfied by beam eigenfunctions, Warburton's formulas are

approximate expressions for this type of boundary. Its accuracy in predicting the plate eigenfrequencies was studied by Leissa (1973) and the validity of using these approximate eigenfunctions for predicting the response of the proposed building model is studied in the results section.

Floor-columns coupling

The coupling of the columns with the floor is performed imposing that the displacement of both systems at the coupling positions is equal. The required floor deflections are obtained by substituting in Eq. (7) the position of all the columns. Using the following definitions

$$\begin{aligned} \mathbf{W}_k &= \left\{ W_k(x_1,y_1) \quad \dots \quad W_k(x_1,y_{N_y}) \quad W_k(x_2,y_1) \quad \dots \quad W_k(x_{N_x},y_{N_y}) \right\}^T, \\ \mathbf{F}_k &= \left\{ F^k_{1,1} \quad \dots \quad F^k_{1,N_y} \quad F^k_{2,1} \quad \dots \quad F^k_{N_x,N_y} \right\}^T \end{aligned} \tag{10}$$

and taking into account the forces applied in each floor (see Fig. 3), the deflections of any intermediate floor k and the deflections of the roof (where $k = N_s + 1$) can be expressed as

$$\mathbf{W}_k = \mathbf{A}(\mathbf{F}_{2k-1} - \mathbf{F}_{2k}), \qquad \mathbf{W}_{N_s+1} = \mathbf{A}\mathbf{F}_{2N_s+1}, \tag{11}$$

where

$$\mathbf{A} = \begin{bmatrix} A(x_1,y_1;x_1,y_1) & \dots & A(x_1,y_1;x_{N_x},y_{N_y}) \\ \vdots & & \vdots \\ A(x_{N_x},y_{N_y};x_1,y_1) & \dots & A(x_{N_x},y_{N_y};x_{N_x},y_{N_y}) \end{bmatrix}. \tag{12}$$

In the case of the ground floor, where $k = 0$, the deflection is given by

$$\mathbf{W}_0 = \mathbf{A}_p\mathbf{F}_p - \mathbf{A}\mathbf{F}_0, \tag{13}$$

where $\mathbf{F}_p$ are the building-pile coupling forces, which will be defined in the next subsection, and $\mathbf{A}_p$ is the matrix of floor compliances at the piles positions. For the sake of simplicity, it will be assumed that the piles and columns positions are the same and, therefore, $\mathbf{A} = \mathbf{A}_p$.

In the case of the columns, defining

$$\mathbf{U}_k(z) = \left\{ U^k_{1,1}(z) \quad \dots \quad U^k_{1,N_y}(z) \quad U^k_{2,1}(z) \quad \dots \quad U^k_{N_x,N_y}(z) \right\}^T, \tag{14}$$

the head and base vertical displacements of all the columns in story k can be compactly expressed as

$$\begin{aligned} \mathbf{U}_k(0) &= \mathbf{C}_{00}\mathbf{F}_{2k} + \mathbf{C}_{0L}\mathbf{F}_{2k+1}, \\ \mathbf{U}_k(L_c) &= \mathbf{C}_{L0}\mathbf{F}_{2k} + \mathbf{C}_{LL}\mathbf{F}_{2k+1}, \end{aligned} \tag{15}$$

where

$$\begin{aligned} \mathbf{C}_{0L} &= C_L(0)\mathbf{I} = -C_0(L_c)\mathbf{I} = -\mathbf{C}_{L0}, \\ \mathbf{C}_{LL} &= C_L(L_c)\mathbf{I} = -C_0(0)\mathbf{I} = -\mathbf{C}_{00}, \end{aligned} \tag{16}$$

where $\mathbf{I}$ is the $(N_x \cdot N_y) \times (N_x \cdot N_y)$ identity matrix and where C_0 and C_L are obtained from Eq. (2).

The coupling forces of the building model are obtained considering the following set of conditions: For the roof, the vertical displacement of the top columns is equal to the roof deflection at the floor-column joint positions. Then, $\mathbf{W}_{N_s+1} = \mathbf{U}_{N_s}(L_c)$, and the coupling equations can be expressed as

$$(\mathbf{A} - \mathbf{C}_{LL})\mathbf{F}_{2N_s+1} - \mathbf{C}_{L0}\mathbf{F}_{2N_s} = \mathbf{0}. \tag{17}$$

For any intermediate floor k, the vertical displacement of the base of the upper columns

(Columns k) is equal to the vertical displacement of the top of the lower columns (Columns $k-1$) and equal to the floor deflection at the floor-column joint positions. Then, $\mathbf{W}_k = \mathbf{U}_k(0) = \mathbf{U}_{k-1}(L_c)$, which gives the following set of coupling equations

$$\begin{aligned} \mathbf{C}_{0L}\mathbf{F}_{2k+1} + (\mathbf{C}_{00} + \mathbf{A})\mathbf{F}_{2k} - \mathbf{A}\mathbf{F}_{2k-1} &= \mathbf{0}, \\ \mathbf{C}_{0L}\mathbf{F}_{2k+1} + \mathbf{C}_{00}\mathbf{F}_{2k} - \mathbf{C}_{LL}\mathbf{F}_{2k-1} - \mathbf{C}_{L0}\mathbf{F}_{2k-2} &= \mathbf{0}. \end{aligned} \tag{18}$$

For the ground floor, the vertical displacement of the base of the columns is equal to the ground floor deflection at the floor-column joint positions. Then, $\mathbf{W}_0 = \mathbf{U}_0(0)$, and the coupling equation can be expressed as

$$\mathbf{C}_{0L}\mathbf{F}_1 + (\mathbf{C}_{00} + \mathbf{A})\mathbf{F}_0 - \mathbf{A}\mathbf{F}_p = \mathbf{0}. \tag{19}$$

Soil-pile model

The proposed building-soil coupled model considers piled foundations in a horizontally stratified soil. For representing the soil-pile interaction, Novak (1974) presented an analytical approach of the system based on linear elasticity. A more accurate solution, which also considered the pile-soil-pile interaction (PSPI), was developed by Kaynia and Kausel (1982, 1991). The main disadvantage of their formulation is the computational cost required to obtain the response for a large set of piles. An efficient alternative, for the case of homogeneous half-spaces, has been presented by Kuo and Hunt (2013a). The same authors have recently published a review of the dynamic models proposed for predicting the response of piled foundations (Kuo and Hunt 2013b).

Since the computational efficiency of the model is a priority, the dynamic soil-pile interaction is represented in this work using the Novak pile model for the case of a layered half-space. This model accounts for the soil-pile interaction considering that the soil is composed of independent infinite horizontal layers of infinitesimal width and assuming that the pile can only move in a vertical plane. The model takes into account the soil inertia

and the dissipation of energy due to radiation damping. The Novak model is used, first, to obtain the response of each pile to an incident ground wavefield and, after, to obtain the pile-cap driving point response. For both calculations Kuo (2010) presented several comparisons between the results obtained using this model and those obtained using more accurate but less efficient alternatives. The comparisons show that the Novak pile model makes a very good prediction of the vertical driving point response of a pile-head. However, when an underground railway-induced incident wavefield is considered, the model shows a significant loss of precision predicting the pile-head response for some ranges of excitation frequencies. The results also show that, when two-pile or four-pile rows are considered, the deviation between the response predicted by the Novak pile model and that of a BE model of the system is negligible for low excitation frequencies and does not exceed 10 dB for the whole frequency range of interest.

The previous results indicate that the use of the Novak pile model introduces a certain loss of precision in the proposed model but, for many applications, this reduction is clearly compensated by the simplicity of its formulation and the efficiency of its computation.

Incident wavefield response

The Novak pile model response to an incident wavefield is computed using the formulation presented in (Kuo 2010). The pile-head vertical response is obtained by discretizing the pile length into N_p equal segments and considering that the soil-pile interaction forces are action-reaction forces applied at the ends of these segments (see Fig. 4). Since the PSPI is not taken into account, it is assumed that the coupling forces caused by pile i do not affect the response of pile $j \neq i$.

The soil and pile responses $\mathbf{U}_s$ and $\mathbf{U}_p$ can be expressed as

$$\mathbf{U}_s = \mathbf{H}^s \mathbf{F}_{ps} + \mathbf{U}_{s,iw}, \qquad \mathbf{U}_p = -\mathbf{H}^p \mathbf{F}_{ps}, \tag{20}$$

where $\mathbf{U}_{s,iw}$ is the incident wavefield and where $\mathbf{H}^s$ and $\mathbf{H}^p$ are the soil and pile compliance

matrices, respectively. These matrices contain, for each subsystem, the response at the N_p discretized positions to forces applied on them. The soil response is obtained allowing no relative motion between the piles and the soil and ignoring the effect of the pile cavities. The resulting expression is

$$\mathbf{U}_p = (\mathbf{H}^s(\mathbf{H}^p)^{-1} + \mathbf{I})^{-1}\mathbf{U}_{\mathrm{s,iw}}, \tag{21}$$

where $\mathbf{I}$ is a $N_p \times N_p$ identity matrix.

The matrix $\mathbf{H}^p$ is obtained by computing the axial response of a thin rod with free-end boundary conditions to axial forces applied on it. Its analytical expression can be found in (Kuo 2010).

The matrix $\mathbf{H}^s$, which is obtained using the approximation developed by Baranov (1967), is a diagonal matrix of the following form

$$\mathbf{H}^s = \frac{1}{(L_p/N_p)} \begin{pmatrix} \ddots & & \\ & \mu_i S_{z,i} & \\ & & \ddots \end{pmatrix}, \tag{22}$$

where μ_i is the shear modulus of layer i, L_p is the length of the pile and where the expression $S_{z,i}$ can be found in (Novak 1974).

The incident wavefield $\mathbf{U}_{s,iw}$ is computed using the Stiffness Matrix Method (SMM) presented by Kausel and Röesset (1981), which considers that the soil is a horizontally stratified isotropic linear elastic media. In the SMM the response of the soil is obtained by transforming the problem to the wavenumber-frequency domain, where the force and the response are related by simple algebraic equations. In this work it is assumed that the system is excited by a vertical harmonic circular force applied either on the surface or at a certain depth in the layered half-space. In cylindrical coordinates the components p_r, p_θ and p_z of the force can be expressed as

$$p_z(r,z,t) = P_0 H(r_{\text{load}} - r)\delta(z - z_{\text{load}})\mathrm{e}^{\mathrm{i}\omega t}, \qquad p_\theta = p_r = 0, \tag{23}$$

where r_{load} is the load radius, z_{load} is the load depth, P_0 is the load amplitude, H is the Heaviside function and δ is the Dirac's delta function.

Applying a Hankel transform in r and a Fourier series decomposition in θ, the transformed force coefficients $\bar{P}_n$ are expressed as

$$\bar{P}_{0,j}(k,\omega) = \frac{1}{2\pi}\int_0^{r_{\text{load}}} r J_0(kr)\mathrm{d}r, \qquad \bar{P}_{n>0,j}(k,\omega) = 0. \tag{24}$$

where j refers to the interface $z = z_{\text{load}}$ where the load is situated.

The response at each soil interface is obtained by inverting, for each value of n, k and ω, the following system of equations

$$\bar{\mathbf{P}} = \mathbf{K}_{\text{system}}\bar{\mathbf{U}} \tag{25}$$

where the vectors $\bar{\mathbf{P}}$ and $\bar{\mathbf{U}}$ contain the applied loads and the resulting displacements at each interface. The response at each one of the piles discretized positions is obtained from the interfaces responses using the analytic continuation of the soil.

The vertical soil response in the space-frequency domain is finally obtained by applying an inverse Hankel transform to the wavenumber response using

$$\mathbf{U}_z(r,\omega) = \frac{1}{2\pi}\int_0^{\infty} \bar{\mathbf{U}} k J_0(kr)\mathrm{d}k. \tag{26}$$

More details regarding the outlined procedure can be found in (Kausel 2006).

The response of all building pile-heads to an incident wavefield is obtained by computing the first row of Eq. (21) for each one of the piles. Following the previous definitions, the resulting displacements can be compactly expressed as

$$\mathbf{U}_{ph}^{\text{ext}} = \left\{ U_p(x_1, y_1, 0) \quad \dots \quad U_p(x_1, y_{N_y}, 0) \quad U_p(x_2, y_1, 0) \quad \dots \quad U_p(x_{N_x}, y_{N_y}, 0) \right\}^T. \tag{27}$$

Driving point response

A pile buried in a layered half-space interacts with N_{int} soil layers. The Novak pile model assumes that, for $i = 1, \dots, N_{\text{int}}$, the vertical response of the pile can be expressed as

$$U_i^p(z) = A_i \sin(\beta_i z) + B_i \cos(\beta_i z), \qquad z_i \leq z \leq z_{i+1}, \tag{28}$$

where z_i and z_{i+1} are the depths of the upper and lower interfaces of the layer, respectively, and

$$\beta_i^2 = \frac{\rho_p A_p \omega^2 - \mu_i S_{z_i}}{E_p A_p}, \tag{29}$$

where E_p is the Young modulus of the pile material, A_p is its section and ρ_p is its density.

The constants A_i and B_i are determined considering the following set of boundary conditions: the pile-top is excited by a vertical harmonic load F_p, the pile-bottom is assumed to be free and the pile vertical displacements and stresses are assumed to be continuous at each layer interface. This set of conditions can be expressed as

$$\begin{aligned} \left.\frac{\mathrm{d}U_1^p}{\mathrm{d}z}\right|_0 &= \frac{F_p}{E_p A_p}, & \left.\frac{\mathrm{d}U_{N_{\text{int}}}^p}{\mathrm{d}z}\right|_{L_p} &= 0, \\ \left.U_i^p\right|_{z_{i+1}} &= \left.U_{i+1}^p\right|_{z_{i+1}}, & \left.\frac{\mathrm{d}U_i^p}{\mathrm{d}z}\right|_{z_{i+1}} &= \left.\frac{\mathrm{d}U_{i+1}^p}{\mathrm{d}z}\right|_{z_{i+1}}. \end{aligned} \tag{30}$$

Once the coefficients A_i and B_i are determined, the driving point response of each pile is given by Eq. (28) when $z = 0$ and the driving point response of all the pile-heads can be compactly written as

$$\mathbf{U}_{ph}^{dp} = H^{ph}\mathbf{I}\mathbf{F}_p, \tag{31}$$

where H^{ph} is the compliance of each pile-head to a force applied on it and where $\mathbf{F}_p$ is a vector that contains the forces applied on all the pile-heads. For the sake of simplicity the piles have been arranged in the same rectangular grid pattern considered for the building columns.

Building-piles coupling

The building-soil model is obtained by coupling the soil-pile system to the building ground floor. The vertical displacement of the pile-heads is a combination of the driving point response, obtained with Eq. (31), and the response to an incident wavefield, obtained with Eq. (27). This response can be expressed as

$$\mathbf{U}_{ph} = \mathbf{U}_{ph}^{dp} + \mathbf{U}_{ph}^{\text{ext}} = H^{ph}\mathbf{I}\mathbf{F}_p + \mathbf{U}_{ph}^{\text{ext}}. \tag{32}$$

The building-piles coupling is performed considering, first, that the vertical displacement of the pile-heads is equal to the vertical displacement of the building ground floor and, second, that this pile-heads displacement is equal to the vertical displacement of the base of the ground columns (see Fig 5). Then, $\mathbf{W}_0 = \mathbf{U}_0(0)$, $-\mathbf{U}_{ph} = \mathbf{W}_0$ and the resulting equations are

$$\begin{aligned} \mathbf{C}_{0L}\mathbf{F}_1 + (\mathbf{C}_{00} + \mathbf{A})\mathbf{F}_0 - \mathbf{A}\mathbf{F}_p &= \mathbf{0}, \\ -\mathbf{A}\mathbf{F}_0 + (\mathbf{A} + H_p\mathbf{I})\mathbf{F}_p &= -\mathbf{U}_{ph}^{\text{ext}}. \end{aligned} \tag{33}$$

The coupling loads between the different subsystems (columns, floors and piles) are obtained combining Eqs. (17), (18) and (33). For the case where the building model is not coupled to the soil, the only difference is that the last equation is replaced with Eq. (19). As an example, the matrix equation obtained for a three-story building is detailed in Appendix A. Once the coupling loads are known, the response of the building floors is

obtained using Eqs. (11) and (13).

RESULTS

This section discusses some significant results obtained using the presented model. The section has been divided into two parts, one presenting results obtained with the building model without soil and foundations and another with the complete building-soil coupled model.

Building model

The floor response predicted by the proposed building model formulation has been compared to the one obtained with a 3D FE model. The comparison has been performed considering two three-story buildings consisting of a ground floor, two upper floors and a roof, joined with a regular grid of circular columns. In the x-direction the grid has 6 columns in the case of the first building and 13 columns in the case of the second one. In both buildings, 3 columns have been considered in the y-direction. The separation between the center of two consecutive columns is 4.5 m in the x-direction and 3 m in the y-direction. In both directions, the distance between the center of the first or last columns and the floor edge in that direction is 0.5 m. The mechanical parameters considered for representing the floors as thin plates and the columns as thin rods are presented in Tables 1 and 2.

The numerical model of the buildings uses 8-node hexahedral elements for meshing the floors and 6-node wedge elements for meshing the columns. A length of approximately 0.15 m has been considered for both types of elements, which ensures that the bending waves of the floors are meshed with more than ten elements per wavelength for the whole range of frequencies of interest. The numerical model of the first building case, which has been presented in Fig. 6, has a total of 42,432 hexaedral elements and 6,804 wedge elements. In the case of the second building, the mesh consists of 57,408 hexaedral and 16,614 wedge elements.

In both models, the building has been excited by applying a vertical harmonic unitary point load at each node of all the pile-cap positions. The same input force has been considered

for the case of the proposed new semianalytic model. The modal response of the thin plate has been computed considering a truncation frequency of 400 Hz, which satisfies the Rubin criterion (Rubin 1975). The comparison has been performed considering a frequency resolution of 0.2 Hz between 1 and 80 Hz. The results have been presented as acceleration levels

$$L_{\ddot{W}} = 20\log_{10}\left(\frac{|\ddot{W}|}{\ddot{W}_{\text{ref}}}\right) = 20\log_{10}\left(\frac{\omega^2|W|}{\ddot{W}_{\text{ref}}}\right) \tag{34}$$

with a reference value $\ddot{W}_{\text{ref}} = 1$ m/s^2. Because a set of unitary harmonic loads has been considered in all the calculations, the presented responses can be also understood as accelerances $H_a(\omega) = \ddot{W(\omega)}/F$ of the considered load configuration.

The results presented in Fig. 7 compare the absolute response of the numerical model with the response of the proposed model at two arbitrary positions of the first building. A good agreement has been found between both responses. A small shift can be observed in the position of some of the building modes, which can be explained observing the results presented in (Leissa 1973), where the eigenfrequecies computed using Warburton's expressions are compared with those found using more accurate solutions. A good agreement is also observed between the amplitudes of a large majority of the modes, ensuring the validity of the approximations performed in the proposed model. The use of the absolute response instead of the vertical one for the numerical model also ensures that, for the considered loading conditions, the horizontal floor responses are much inferior than the vertical ones. The running time to obtain the results shown in Fig. 7 with the new analytical model, which has been computed using MATLAB interpreted code, is about 40 seconds on a personal computer equipped with a 3.16GHz Intel Core 2 Duo processor and 4 Gb of RAM. Around 75 minutes were required to obtain the results with the numerical model, which has been developed using the MSC NASTRAN finite element software.

As can be seen in Fig. 8, a similar agreement has been obtained in the predicted responses for the second building. Again, the comparison has been performed for two different nodes.

The proposed building model can be used to obtain insights of the floors' dynamic behavior and to predict the efficiency of several vibration countermeasures. Fig. 9 studies the influence that considering a thicker lower floor has on the building vertical vibration. This case has been previously addressed by Sanayei et al. (2012, 2014) using a one-dimensional modified column model. Due to the considered assumptions, the model used in their works does not take into account the dynamical behavior of a finite floor and predicts the vibration response at the base of a building column. In contrast, the building model presented in this work allows extending their study to any position of the building floors. In particular, the response at the center of each floor is considered in these results. A width of 1.2 m has been considered in the thicker lower floor case instead of the 0.3 m used in the normal floor. It should be mentioned that the use of a different floor width requires computing the ground floor compliance $A(x, y; x_i, y_j)$ of each floor separately. Again, the results have been computed using a 0.2 Hz resolution from 1 to 80 Hz.

The results show that floor responses are considerably modified by a change in the thickness of the floor. Although an increase of the vibration response can be observed for certain excitation frequencies, the floor response is clearly reduced in most of the studied frequency range. The vibration attenuation has been quantified in Table 3, which shows the total reduction obtained using this countermeasure in the range of frequencies studied. The total reduction has been computed applying the frequency weighting described in (International Organization for Standardization 2003), which specially reduces the amplitude of the high-frequency content of the response. The presented values can be understood as the difference between the obtained building vibration levels when the spectrum of the applied force is equal to the one of a white noise from 1 to 80 Hz. As it could be expected, this vibration countermeasure is specially effective for the ground floor, which has been significantly stiffened by the increase of its thickness. The reduction obtained in this study is smaller than the one presented in Sanayei et al. (2014). In their case, however, the reduction was computed considering the building velocity of vibration levels due to a railway-induced

excitation for a wider range of excitation frequencies.

An alternative potential vibration countermeasure is the use of columns with larger cross-sections. This option has been studied comparing the floor response for two column radius: 0.15 m and 0.3 m. As Fig. 10 shows, the responses are also significantly affected by this geometrical modification and they are again reduced for most of the studied range. As before, the efficiency of this countermeasure has been quantified in Table 3, which shows that, for the upper building floors, the reduction in the vibration levels obtained using columns with a larger cross-section is higher than the one obtained using a thicker lower floor.

The use of a thicker lower floor or of columns with a larger cross-section has been also considered for the second building model. The obtained global reductions for this case, which are presented in Table 4, are slightly inferior than the ones obtained for the first building but, again, the results indicate that the use of columns with a larger cross-section is a better vibration countermeasure for the upper building floors.

Building-soil model

The building-soil coupled model is finally used for showing the effect that the soil stratification has on the building floors response. The results presented in Fig. 11 have been obtained coupling the first of the previous building models to a soil consisting of two horizontal layers over a half-space. The same spatial rectangular grid pattern has been considered for the columns and for the piles. The comparison has been performed considering two soils that only differ in the stiffness of their upper layer. In the first case, this layer is very soft, with a Young modulus $E_s = 20$ MPa. In the second case, the layer is considerably stiff, with $E_s = 150$ MPa. The mechanical parameters considered for the piles and for each layer are presented in Tables 5 and 6. The incident wavefield has been computed using a vertical harmonic load with a circular surface distribution, a radius $r_m = 0.25$ m and situated at $(x_m, y_m) =$ (-5,-5) m in the floors system of coordinates presented in Fig. 2. The building-soil configuration considered is similar to the one initially presented in Fig. 1 but with a larger building and with the load applied in a different position. The computation of the

SMM in cylindrical coordinates requires evaluating a numerical inverse Hankel transform. This transform has been performed using a logarithmical sampling with 2,048 samples and convergence tests have been carried out to ensure the accuracy of the results. As in the previous section, the modal response of the thin plate has been computed considering a truncation frequency of 400 Hz. The correctness of the pile and soil numerical computations have been tested reproducing the results presented in (Kuo 2010), for the Novak model response, and in (Kausel 2006) for the SMM response. The correctness of the Novak pile formulation for a layered half-space has been tested comparing the results obtained for a certain soil stratification with those obtained when the layers of this stratification are divided in smaller equal layers. The pile length has been discretized ensuring that five nodes per wavelength are used when the frequency of the external excitation is 80 Hz. The wavelength considered is the one related to the shear wave speed of the soil upper layer.

The results show that the vertical response of the building floors clearly depends, for the whole range of frequencies of interest, on the type of soil stratification considered. Significant differences have been found not only in the amplitude of all floors response but also in the frequencies where the peaks of this response occurs. The results indicate that the resonances of the system are shifted to lower frequencies when a very soft upper layer is considered instead of a stiff one, a result that is in agreement with the fact that a reduction in the soil flexibility tends to increase the resonance frequencies of the building (Jennings 1973). It can be also observed that for both types of soil the low-frequency response of all floors is considerably more damped than the high-frequency one. Additionally, while the response of the building on a softer soil tends to decrease as the excitation frequency increases, the opposite tendency occurs for the building on a stiffer soil. It is therefore concluded that the SSI has to be taken into account for the type of soils considered in this work.

Rather than performing a detailed quantification of the SSI effect, the aim of the previous comparison is to highlight the importance of having the soil parameters well characterized for performing accurate predictions of the building response to ground-borne vibrations.

The efficiency of the proposed model is especially useful for cases where these characterization presents a considerable uncertainty and a large amount of prediction calculations are required.

DISCUSSION

The building-soil coupled model for predicting the response of a N-storey building with rectangular floors to ground-borne vibrations presents two main advantages against a FE model of the problem. First, the proposed formulation is significantly more computationally efficient than a FE one. This efficiency has been previously detailed for the building results but is even more clear for the case of the coupled building-soil model. It is well-known that, for the range of frequencies of interest, a 3D numerical model of this system requires very large computational costs, even when alternative modelling techniques, such as the use of a FE-BE hybrid formulation, are used. The second advantage of the presented model is its simplicity for dealing with different building configurations. Parameters such as the number of stories, the number and the geometrical distribution of columns in each floor or the value of the mechanical properties of each element are simply numerical inputs on the model. Therefore, the time-consuming FE preprocessing tasks are avoided. This advantage is particulary important if the vibration response of a considerable number of different buildings (or building configurations) needs to be assessed.

Due to the assumptions performed, the model has certain applicability limitations that should be pointed out. Because Warburton (1954) approximate expressions are considered for computing the floor responses, the model cannot be used for predicting the response of buildings with non-rectangular floors. In such cases, the presented model can still be used for performing large-scale predictions in an early design stage and more accurate predictions for specific sites can be later obtained using alternative numerical models. Regarding the building foundations, the model assumes pile foundations and, therefore, it is not suitable for predicting the response of buildings with other types of foundations, such as footings or raft foundations. However, it should be pointed out that this drawback can be overcome by

modifying some of the considered hypothesis of the model. Finally, the model is focused to predict the vertical component of the building vibration, which is, for the type of induced vibrations considered, the main component of the floor's response.

CONCLUSIONS

This paper presents a computationally efficient three-dimensional building-soil coupled model for predicting the response of a building to ground-borne vibrations. The model considers that the vibration is transmitted to the floors through the building columns and that the vertical component of this vibration is the dominant one. The coupling of the building and the soil has been performed considering piled foundations and a horizontally stratified soil. They have been modeled using the Novak pile model and the SMM for a layered half-space, respectively. The use of a simplified soil-pile model ensures the simplicity and efficiency of the model and allows to take into account the effect of soil stratification. The presented model is highly suitable for performing many types of parametric studies and large-scale vibration predictions due to its small computational cost and considerable accuracy.

The response of the building model has been compared to the one obtained using a FE model of two different three-story building examples, finding a good agreement between both in the range of frequencies of interest in building response to ground-borne vibrations. The building model has been used to study the isolation efficiency of considering, first, a thicker lower floor and, second, columns with a larger cross-section. The results at the center of each floor show that, although both modifications can be considered as vibration countermeasures, the use of columns with a larger cross-section is significantly more effective for the isolation of the building's upper floors.

The building-soil coupled model is finally used to study the effect that the soil stratification has in the vibration response of the building floors. The results obtained for two different soils show clear differences in all the frequency range studied. This result justifies the importance of having the soil elastic parameters correctly characterised and highlights

the importance of considering a stratified soil model in nonhomogeneous soils.

The proposed building-soil coupled model is able to consider many features of the dynamic response of a N-story building in a layered half-space with a very small computational cost. This advantage can be used for obtaining the building response to a wide variety of excitations in cases where the mechanical parameters of the problem are not accurately defined and/or where the results at large areas or for a large set of buildings are required.

ACKNOWLEDGEMENTS

The results presented have been obtained in the frame of ISIBUR project TRA2014-52718-R, "Innovative Solutions for the Isolation of Buildings from Underground Railway-induced vibrations" funded by the Spanish Ministry of Economy and Competitiveness. This financial support is gratefully acknowledged.

REFERENCES

Athanasopoulos, G. and Pelekis, P. (2000). "Ground vibrations from sheetpile driving in urban environment: measurements, analysis and effects on buildings and occupants." *Soil Dyn Earthq Eng*, 19(5), 371–387.

Auersch, L. (2008). "Dynamic stiffness of foundations on inhomogeneous soils for a realistic prediction of vertical building resonance." *J Geotech Geoenviron*, 134(3), 328–340.

Auersch, L. (2010a). "Technically induced surface wave fields, part I: Measured attenuation and theoretical amplitude-distance laws." *B Seismol Soc Am*, 100(4), 1528–1539.

Auersch, L. (2010b). "Technically induced surface wave fields, part II: Measured and calculated admittance spectra." *B Seismol Soc Am*, 100(4), 1540–1550.

Baranov, V. A. (1967). "On the calculation of excited vibrations of an embedded foundation (in Russian)." *Vopr Dyn Prochn*, 14, 195–209.

Crispino, M. and D'Apuzzo, M. (2001). "Measurement and prediction of traffic-induced vibrations in a heritage building." *J Sound Vib*, 246(2), 319–335.

Cryer, D. P. (1994). "Modelling of vibration in buildings with application to base isolation." Ph.D. thesis, University of Cambridge.

510 Fiala, P., Degrande, G., and Augusztinovicz, F. (2007). "Numerical modelling of ground-
511 borne noise and vibration in buildings due to surface rail traffic." *J Sound Vib*, 301,
512 718–738.
513 Fiala, P., Gupta, S., Degrande, G., and Augusztinovicz, F. (2008). "A numerical model for
514 re-radiated noise in buildings from underground railways." *Note N Fl Mech Mul D*, Vol. 99,
515 115–121.
516 Hood, R., Greer, R., Breslin, M., and Williams, P. (1996). "The calculation and assessment
517 of ground-borne noise and perceptible vibration from trains in tunnels." *J Sound Vib*,
518 193(1), 215–225.
519 Hudson, D. (1956). "Response spectrum techniques in engineering seismology." *Proc World*
520 *Conference on Earthquake Eng.*
521 Hunt, H. E. M. (1995). "Prediction of vibration transmission from railways into buildings
522 using models of infinite length." *Vehicle Syst Dyn*, 24, 234–247.
523 Jennings, P., Bielak, J. (1973). "Dynamics of building-soil interaction." *B Seismol Soc Am*,
524 63(1), 9–48.
525 Hussein, M., Hunt, H., Kuo, K., Alves Costa, P., and Barbosa, J. (2013). "The use of sub-
526 modelling technique to calculate vibration in buildings from underground railways." *P I*
527 *Mech Eng F-J Rai*, 229(3), 303–314.
528 International Organization for Standardization (2003). *ISO 2631-2:2003 Mechanical vibra-*
529 *tion and shock. Evaluation of human exposure to whole-body vibration. Part 2: Vibration*
530 *in buildings (1 Hz to 80 Hz).*
531 International Organization for Standardization (2005). *ISO 14837-1:2005 Mechanical vibra-*
532 *tion. Ground-borne noise and vibration arising from rail systems.*
533 Jean, P. and Villot, M. (2000). "Study of the vibrational power injected to a wall excited by
534 a ground surface wave." *J Sound Vib*, 231(3), 721–726.
535 Kausel, E. (2006). *Fundamental solutions in elastodynamics: A compendium.* Cambridge
536 University Press.

Kausel, E. and Roësset, J. M. (1981). "Stiffness matrices for layered soils." *B Seismol Soc Am*, 71(6), 1743–1761.

Kaynia, A. M. (1982). "Dynamic stiffness and seismic response of pile groups." Ph.D. thesis, Massachusetts Institute of Technology.

Kaynia, A. M. and Kausel, E. (1991). "Dynamics of piles and pile groups in layered soil media." *Soil Dyn Earthq Eng*, 10(8), 386–401.

Kuo, K. A. (2010). "Vibration from underground railways : Considering piled foundations and twin tunnels." Ph.D. thesis, University of Cambridge.

Kuo, K. A. and Hunt, H. E. M. (2013a). "An efficient model for the dynamic behaviour of a single pile in viscoelastic soil." *J Sound Vib*, 332(10), 2549–2561.

Kuo, K. A. and Hunt, H. E. M. (2013b). "Dynamic models of piled foundations." *Appl Mech Rev*, 65(3), 031003–1–031003–9.

Kuppelwieser, H. and Ziegler, A. (1996). "A tool for predicting vibration and structure-borne noise immissions caused by railways." *J Sound Vib*, 193(1), 261–267.

Kurzweil, L. G. (1979). "Ground-borne noise and vibration from underground rail systems." *J Sound Vib*, 66(3), 363–370.

Leissa, A. W. (1973). "The free vibration of rectangular plates." *J Sound Vib*, 31(3), 357–293.

Lombaert, G., Degrande, G., François, S., and Thompson, D. J. (2015). "Ground-Borne Vibration due to Railway Traffic: A Review of Excitation Mechanisms, Prediction Methods and Mitigation Measures." *Note N Fl Mech Mul D*, Vol. 126, 253–287.

Lopes, P., Alves Costa, P., Calçada, R., and Silva Cardoso, A. (2014). "Influence of soil stiffness on building vibrations due to railway traffic in tunnels: Numerical study." *Comput Geotech*, 61, 277–291.

Madshus, C., Bessason, B., and Hårvik, L. (1996). "Prediction model for low frequency vibration from high speed railways on soft ground." *J Sound Vib*, 193(1), 195–203.

Newland, D. E. and Hunt, H. E. M. (1991). "Isolation of buildings from ground vibration: a review of recent progress." *P I Mech Eng C-J Mec*, 205(1), 39–52.

564 Novak, M. (1974). "Dynamic stiffness and damping of piles." *Can Geotech J*, 11(4), 574–598.
565 Rubin, S. (1975). "Improved component-mode representation for structural dynamic analy-
566 sis." *AIAA J*, 13(8), 995–1006.
567 Sanayei, M., Kayiparambil P., A., Moore, J. A., and Brett, C. R. (2014). "Measurement and
568 prediction of train-induced vibrations in a full-scale building." *Eng Struct*, 77, 119–128.
569 Sanayei, M., Maurya, P., and Moore, J. A. (2013). "Measurement of building foundation and
570 ground-borne vibrations due to surface trains and subways." *Eng Struct*, 53, 102–111.
571 Sanayei, M., Zhao, N., Maurya, P., Moore, J. A., Zapfe, J. A., and Hines, E. M. (2012).
572 "Prediction and mitigation of building floor vibrations using a blocking floor." *J Struct*
573 *Eng-Asce*, 138(10), 1181–1192.
574 Talbot, J. P. (2001). "On the performance of base-isolated buildings: A generic model."
575 Ph.D. thesis, University of Cambridge.
576 Villot, M., Ropars, P., Jean, P., Bongini, E., and Poisson, F. (2011). "Modeling the influence
577 of structural modifications on the response of a building to railway vibration." *Noise*
578 *Control Eng*, 59(6), 641.
579 Waller, R. A. (1969). *Building on springs*. Pergamon press, Oxford.
580 Warburton, G. B. (1954). "The vibration of rectangular plates." *P I Mech Eng*, 168(1),
581 371–384.

582 APPENDIX A.COUPLING LOADS EQUATIONS FOR A THREE-STORY BUILDING

583 This appendix presents the system of equations that has to be computed to obtain the
584 coupling forces for a three-story building. Although this is the only case presented, taller
585 buildings are easily obtained adding new rows and columns of block matrices.

$$\begin{pmatrix} (\mathbf{A}-\mathbf{C}_{LL}) & -\mathbf{C}_{L0} & \mathbf{0} & \mathbf{0} & \mathbf{0} & \mathbf{0} & \mathbf{0} \\ \mathbf{C}_{0L} & (\mathbf{C}_{00}+\mathbf{A}) & -\mathbf{A} & \mathbf{0} & \mathbf{0} & \mathbf{0} & \mathbf{0} \\ \mathbf{C}_{0L} & \mathbf{C}_{00} & -\mathbf{C}_{LL} & -\mathbf{C}_{L0} & \mathbf{0} & \mathbf{0} & \mathbf{0} \\ \mathbf{0} & \mathbf{0} & \mathbf{C}_{0L} & \mathbf{C}_{00}+\mathbf{A} & -\mathbf{A} & \mathbf{0} & \mathbf{0} \\ \mathbf{0} & \mathbf{0} & \mathbf{C}_{0L} & \mathbf{C}_{00} & -\mathbf{C}_{LL} & -\mathbf{C}_{L0} & \mathbf{0} \\ \mathbf{0} & \mathbf{0} & \mathbf{0} & \mathbf{0} & \mathbf{C}_{0L} & \mathbf{C}_{00}+\mathbf{A} & -\mathbf{A} \\ \mathbf{0} & \mathbf{0} & \mathbf{0} & \mathbf{0} & \mathbf{0} & -\mathbf{A} & (\mathbf{A}+H_p\mathbf{I}) \end{pmatrix} \begin{pmatrix} \mathbf{F}_5 \\ \mathbf{F}_4 \\ \mathbf{F}_3 \\ \mathbf{F}_2 \\ \mathbf{F}_1 \\ \mathbf{F}_0 \\ \mathbf{F}_p \end{pmatrix} = \begin{pmatrix} \mathbf{0} \\ \mathbf{0} \\ \mathbf{0} \\ \mathbf{0} \\ \mathbf{0} \\ \mathbf{0} \\ -\mathbf{U}_{ph}^{\text{ext}} \end{pmatrix}.$$

The presented formulation is easy to compute and, unless a great number of columns and stories is considered, very efficient.

List of Tables

TABLE 1: Mechanical parameters used for the floor model.

Parameter	Value
x-direction length (L_x)	16/37 m
y-direction length (L_y)	10 m
Width (h_f)	0.3 m
Young modulus (E_f)	30 GPa
Poisson ratio (ν_f)	0.3
Density (ρ_f)	3000 kg m^{-3}
Structural damping (η_f)	0.02

TABLE 2: Mechanical parameters used for the column model.

Parameter	Value
Height (L_c)	3 m
Radius (r_c)	0.15 m
Young modulus (E_c)	30 GPa
Density (ρ_c)	3000 kg m^{-3}
Structural damping (η_c)	0.02

TABLE 3: Total vibration reduction obtained at the center of each floor in the first building case when the thickness of the lower floor or the size of the columns cross-section are modified.

Countermeasure	Ground f. (dB)	Floor 1 (dB)	Floor 2 (dB)	Roof (dB)
Modified ground floor	12.16	4.73	0.71	1.72
Modified columns	9.09	5.34	5.38	9.11

TABLE 4: Total vibration reduction obtained at the center of each floor in the second building case when the thickness of the lower floor or the size of the columns cross-section are modified.

Countermeasure	Ground f. (dB)	Floor 1 (dB)	Floor 2 (dB)	Roof (dB)
Modified ground floor	12.52	7.26	1.84	3.27
Modified columns	8.42	4.18	4.41	8.56

TABLE 5: Mechanical parameters used for the pile model.

Parameter	Value
Radius (r_p)	0.354 m
Length (L_p)	10 m
Young modulus (E_p)	40 GPa
Density (ρ_p)	2800 kg m^{-3}
Structural damping (η_p)	0.01

TABLE 6: Mechanical parameters used for the soil models.

Parameter	First layer	Second layer	Half-space
Layer thickness (h_s)	5 m	10 m	-
Layer Young modulus (E_s)	20/150 MPa	125 MPa	250 MPa
Layer Poisson ratio (ν_s)	0.3	0.3	0.3
Layer density (ρ_s)	1800 kg m^{-3}	2100 kg m^{-3}	2600 kg m^{-3}
Layer P-wave damping (D_P)	0.03	0.03	0.03
Layer S-wave damping (D_S)	0.03	0.03	0.03

List of Figures

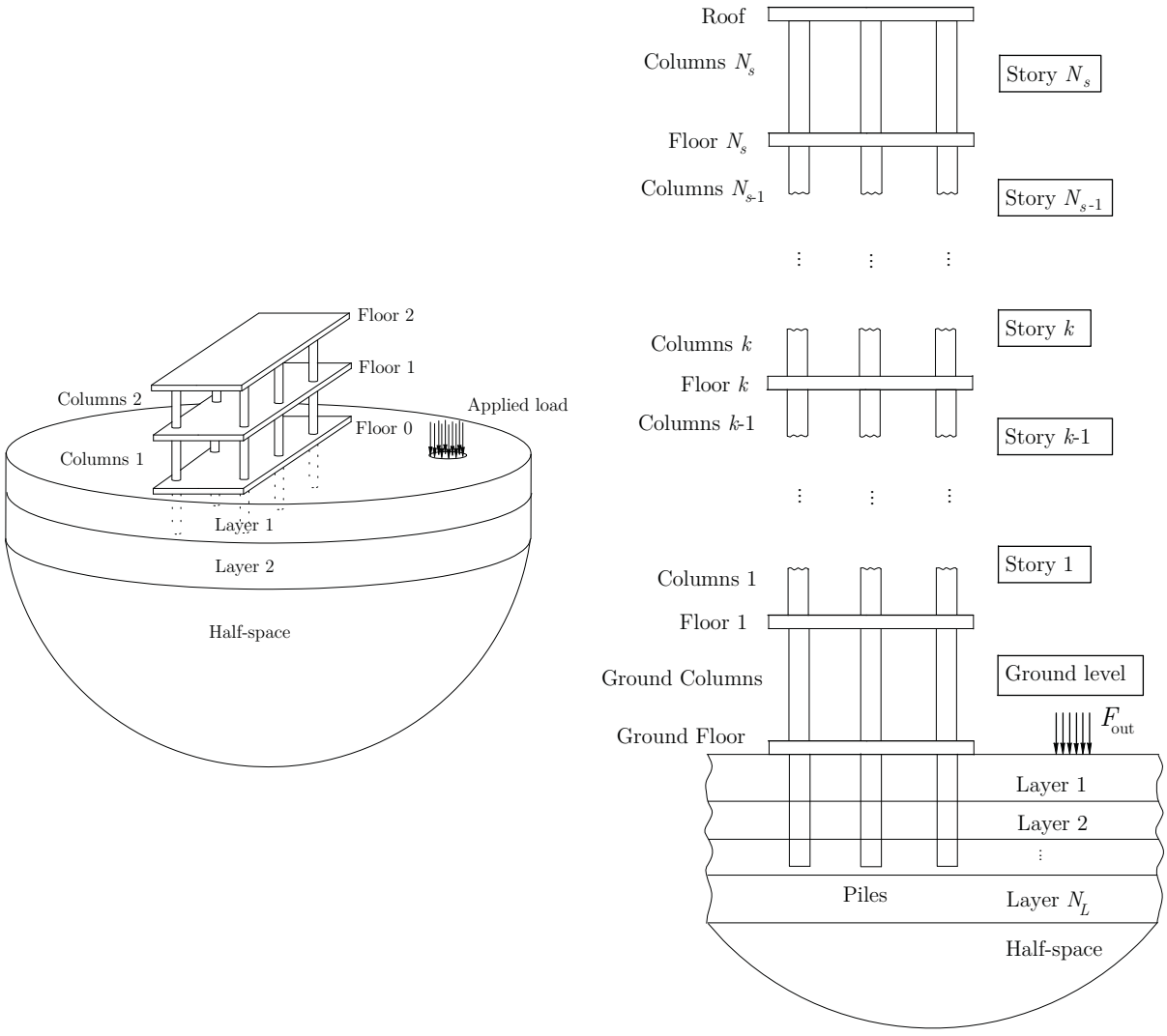
Floor 2
Floor 1
Columns 2
Applied load
Floor 0
Columns 1
Layer 1
Layer 2
Half-space
Roof
Columns N_s
Story N_s
Floor N_s
Columns N_{s-1}
Story N_{s-1}
Columns k
Story k
Floor k
Columns k-1
Story k-1
Columns 1
Story 1
Floor 1
Ground Columns
Ground level
F_{out}
Ground Floor
Layer 1
Layer 2
Piles
Layer N_L
Half-space

(a) (b)

FIG. 1

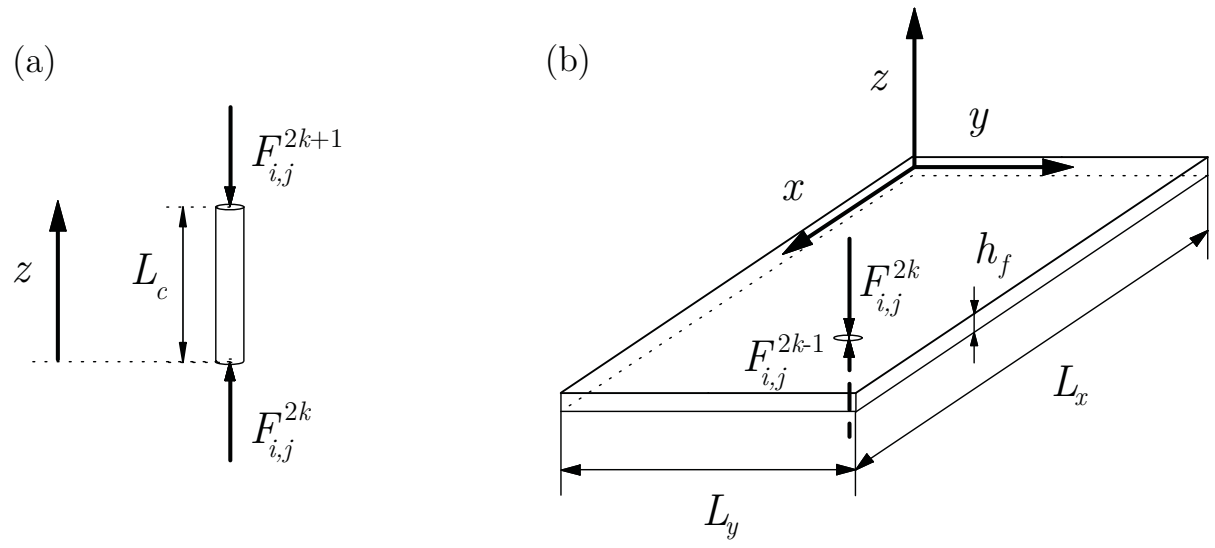

FIG. 2

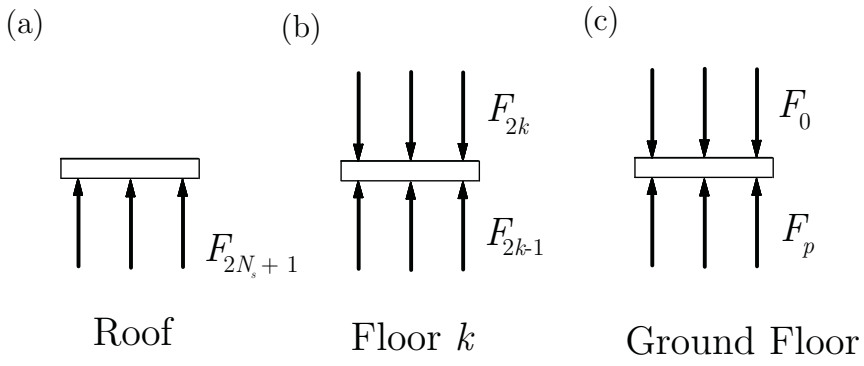

FIG. 3

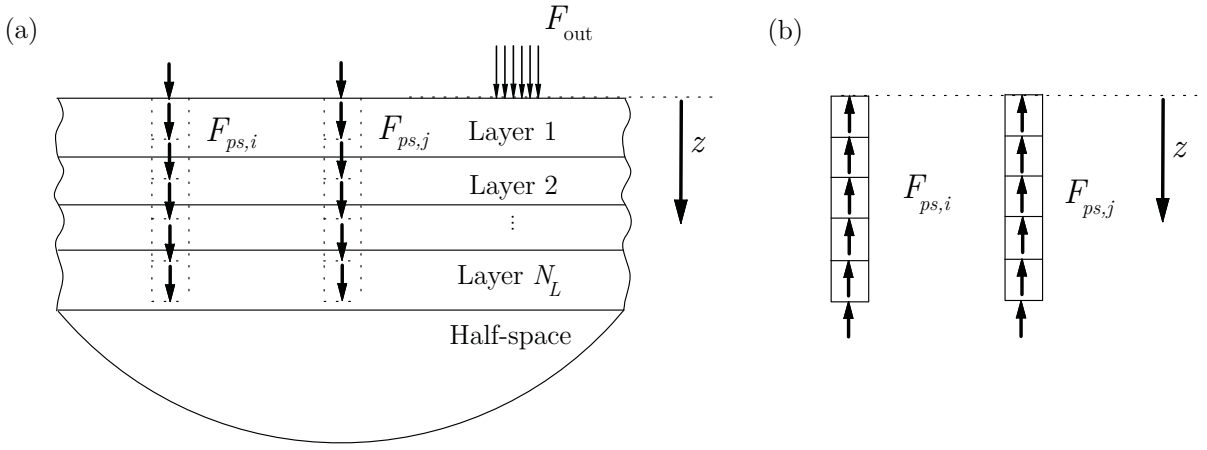
(a)
F_{out}
$F_{ps,i}$
$F_{ps,j}$
Layer 1
Layer 2
Layer N_L
Half-space
z
(b)
$F_{ps,i}$
$F_{ps,j}$
z

FIG. 4

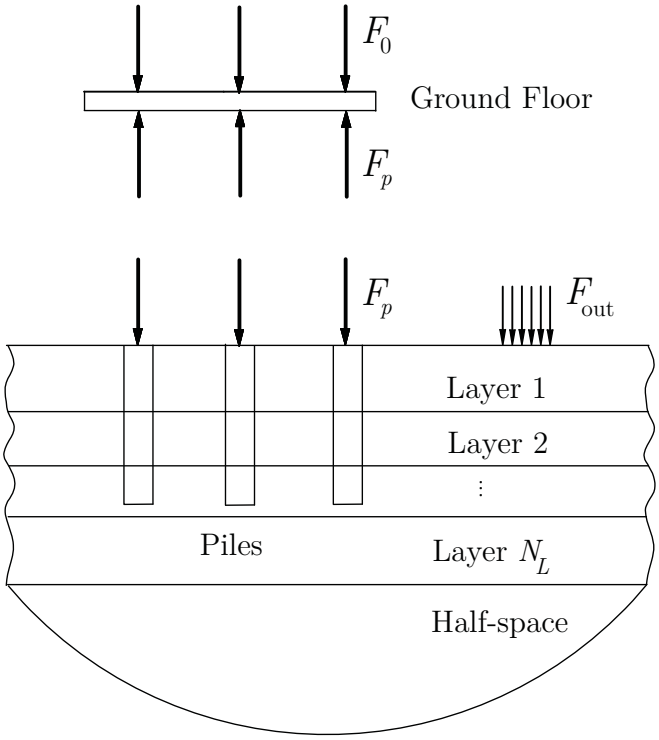
F_0
Ground Floor
F_p
F_p
F_{out}
Layer 1
Layer 2
Piles
Layer N_L
Half-space

FIG. 5

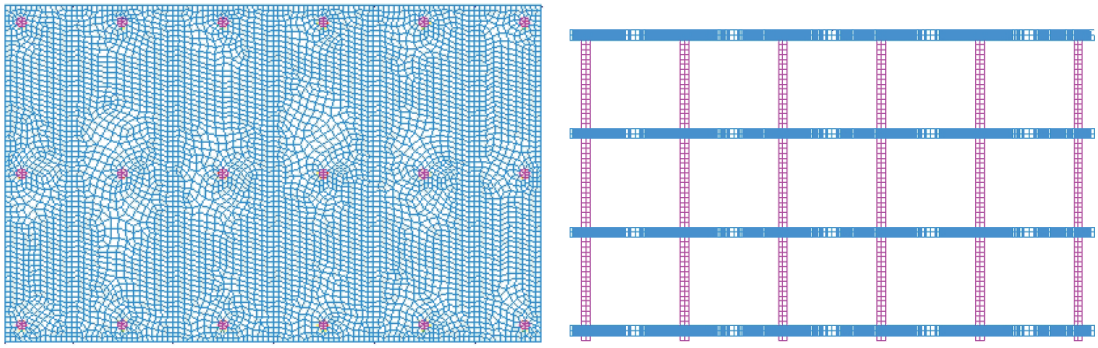

(a) (b)

FIG. 6

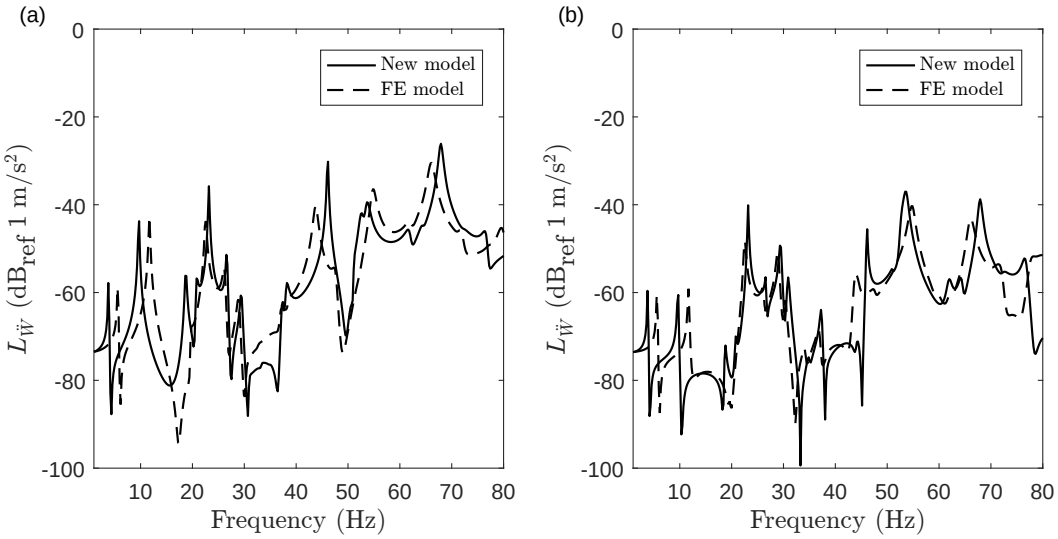
(a)
(b)
New model
FE model
$L_{\ddot{W}}$ (dB$_{\text{ref}}$ 1 m/s^2)
Frequency (Hz)
0
-20
-40
-60
-80
-100
10
20
30
40
50
60
70
80

FIG. 7

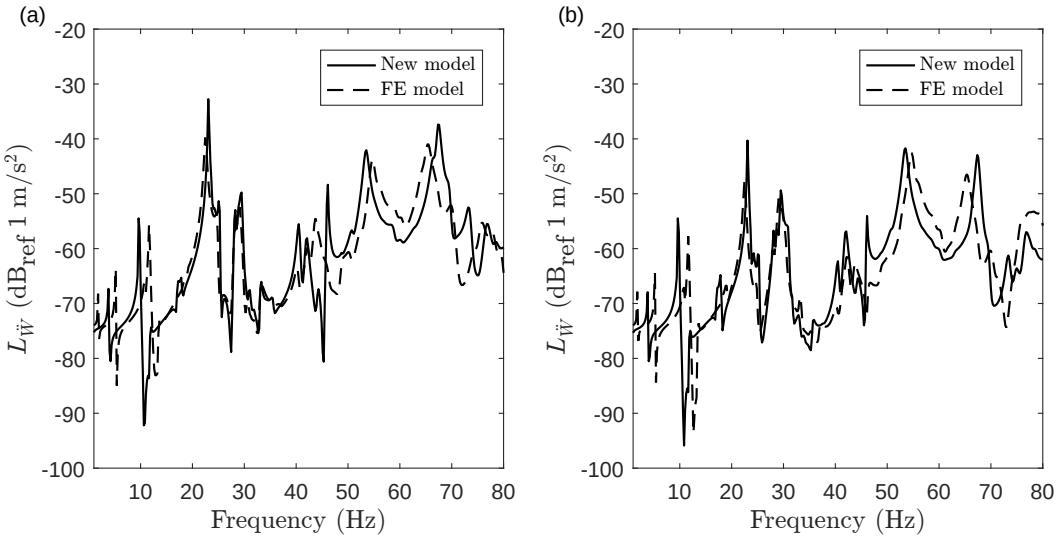
(a)
(b)
New model
FE model
$L_{\ddot{W}}$ (dB$_{\mathrm{ref}}$ 1 m/s^2)
Frequency (Hz)
-20
-30
-40
-50
-60
-70
-80
-90
-100
10
20
30
40
50
60
70
80

FIG. 8

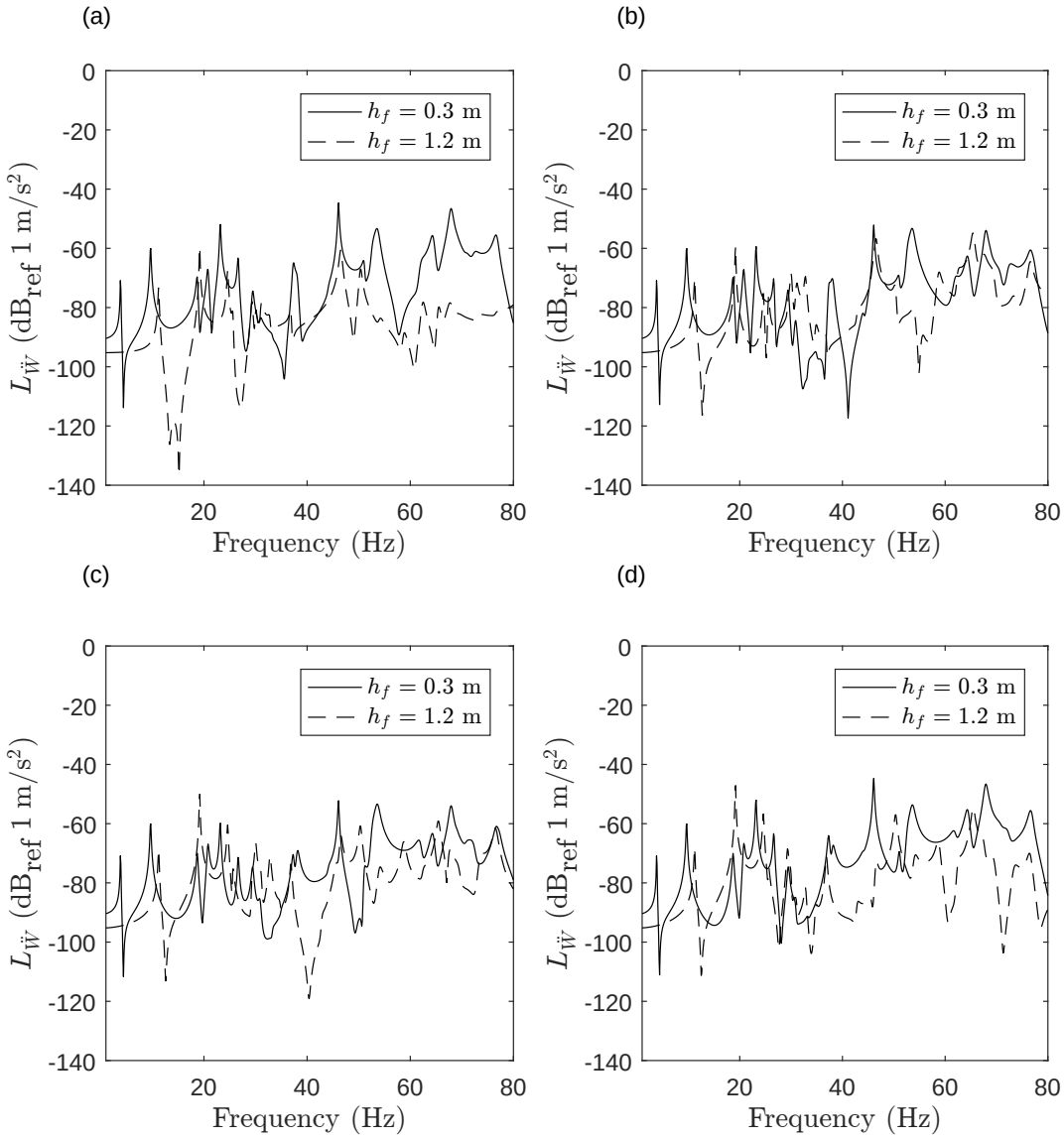
(a)
(b)
(c)
(d)
$h_f = 0.3$ m
$h_f = 1.2$ m
$L_{\ddot{W}}$ (dB$_{\text{ref}}$ 1 m/s^2)
Frequency (Hz)
0
-20
-40
-60
-80
-100
-120
-140
20
40
60
80

FIG. 9

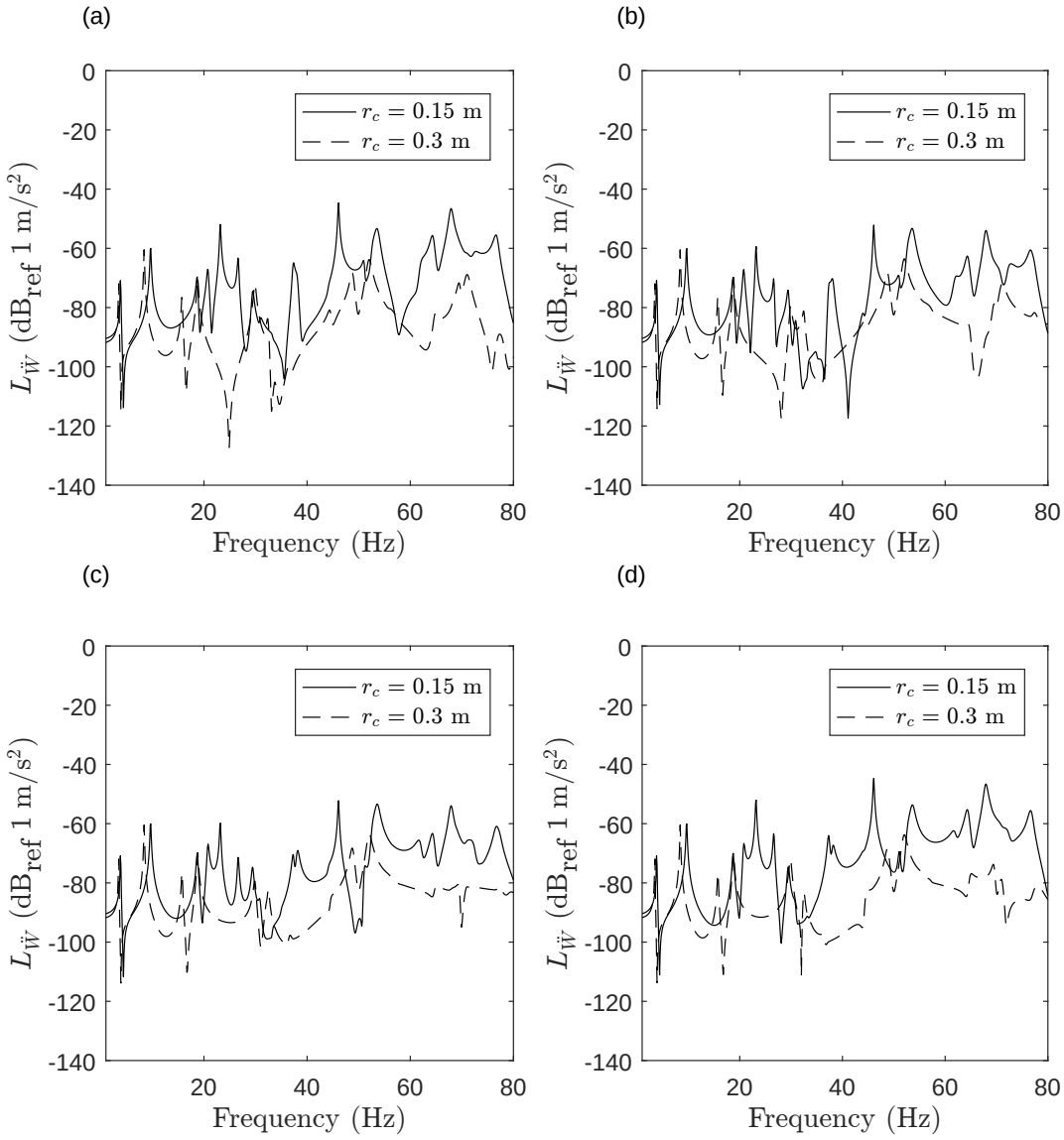
(a)
(b)
(c)
(d)
$r_c = 0.15$ m
$r_c = 0.3$ m
$L_{\ddot{W}}$ (dB$_{\text{ref}}$ 1 m/s^2)
Frequency (Hz)
0
-20
-40
-60
-80
-100
-120
-140
20
40
60
80

FIG. 10

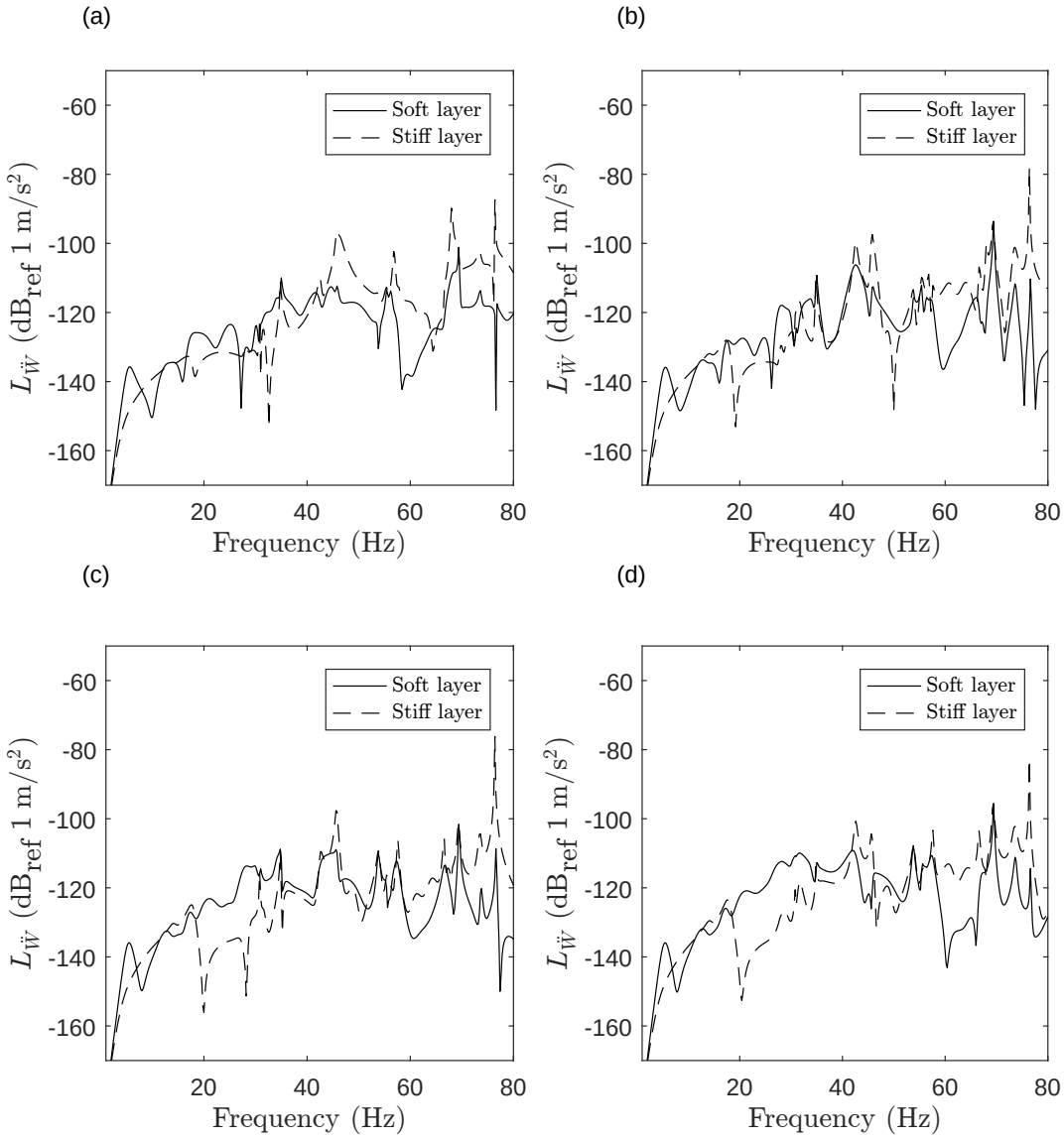
(a)
(b)
(c)
(d)
Soft layer
Stiff layer
$L_{\ddot{W}}$ (dB$_{\mathrm{ref}}$ 1 m/s^2)
Frequency (Hz)
-60
-80
-100
-120
-140
-160
20
40
60
80

FIG. 11